

See discussions, stats, and author profiles for this publication at: <https://www.researchgate.net/publication/231706315>

# Solution-Processable Star-Shaped Photovoltaic Organic Molecule with Triphenylamine Core and Benzothiadiazole-Thiophene Arms

ARTICLE *in* MACROMOLECULES · OCTOBER 2009

Impact Factor: 5.8 · DOI: 10.1021/ma901896n

CITATIONS

104

READS

95

6 AUTHORS, INCLUDING:



Jing Zhang

Fourth Military Medical University

698 PUBLICATIONS 10,035 CITATIONS

SEE PROFILE



Yi Yang

Chinese Academy of Sciences

92 PUBLICATIONS 1,376 CITATIONS

SEE PROFILE



Chang He

Chinese Academy of Sciences

50 PUBLICATIONS 2,050 CITATIONS

SEE PROFILE



Guangjin Zhao

Chinese Academy of Sciences

22 PUBLICATIONS 1,507 CITATIONS

SEE PROFILE

# Solution-Processable Star-Shaped Photovoltaic Organic Molecule with Triphenylamine Core and Benzothiadiazole–Thiophene Arms

Jing Zhang,<sup>†,‡</sup> Yi Yang,<sup>†,‡</sup> Chang He,<sup>†</sup> Youjun He,<sup>†,‡</sup> Guangjin Zhao,<sup>†,‡</sup> and Yongfang Li<sup>\*,†</sup>

<sup>†</sup>Beijing National Laboratory for Molecular Sciences, CAS Key Laboratory of Organic Solids, Institute of Chemistry, Chinese Academy of Sciences, Beijing 100190, China, and <sup>‡</sup>Graduate University of Chinese Academy of Sciences, Beijing 100049, China

Received August 26, 2009

Revised Manuscript Received September 24, 2009

Solution-processable organic molecules have attracted much interest recently for the applications in organic solar cells (OSCs)<sup>1–15</sup> and organic light-emitting diodes (OLEDs)<sup>6,16–19</sup> because of their advantages of high purity and definite molecular weight in comparison with polymers and low-cost solution processability in comparison with vacuum-deposition organic molecules. Triphenylamine (TPA)-containing molecules with D–A structure draw special attention in the applications,<sup>6–10,15–17</sup> for their good solution processability benefited from the three-dimensional propeller structure of TPA and strong visible absorption resulted from the D–A structure. In recent years, our group synthesized a series of TPA-containing molecules with D–A structure for the application in OSCs.<sup>15,20–23</sup> Among the TPA-containing molecules, a star-shaped molecules S(TPA-BT)<sup>15</sup> exhibited a higher power conversion efficiency of 1.33% for the OSC based on S(TPA-BT) as donor blended with PCBM as acceptor.<sup>15</sup>

Here, we synthesized a new star-shaped TPA-containing molecule with TPA as core and benzothiadiazole-(4-hexyl)thiophene as arms, S(TPA-BT-4HT) (see Scheme 1). The end group of 4-hexylthiophene in S(TPA-BT-4HT) instead of TPA end group in S(TPA-BT)<sup>15</sup> is for further improving morphology and photovoltaic property. S(TPA-BT-4HT) shows good solubility in common organic solvents. The film of the compound exhibits broad and strong absorption peaks in the range of 300–630 nm and a red-emission photoluminescent peak at ca. 657 nm. The OSC devices were fabricated by spin-coating the blend solution of S(TPA-BT-4HT) as donor and [6,6]-phenyl-C-71-butyric acid methyl ester ([70]PCBM) as acceptor. The maximum power conversion efficiency (PCE) of an OSC based on a blend of S(TPA-BT-4HT) and [70]PCBM (1:3, w/w) reached 2.39% under the illumination of AM.1.5, 100 mW/cm<sup>2</sup>. The PSC of 2.39% is one of the highest values for the OSCs based on the solution-processable organic molecules reported so far.

S(TPA-BT-4HT) was synthesized by the route shown in Scheme 1. First, 4-bromo-7-(4-hexyl-2-thienyl)-2,1,3-benzothiadiazole (**1**) was synthesized from 4,7-dibromo-2,1,3-benzothiadiazole and tributyl-(4-hexyl-2-thienyl)stannane by Pd(ph<sub>3</sub>)<sub>2</sub>Cl<sub>2</sub>-catalyzed reaction.<sup>24</sup> Then, monomer **2** was prepared according to the method reported in the literature.<sup>21</sup> Finally, S(TPA-BT-4HT) was synthesized from

monomer **1** and monomer **2** by a palladium-catalyzed Heck reaction.

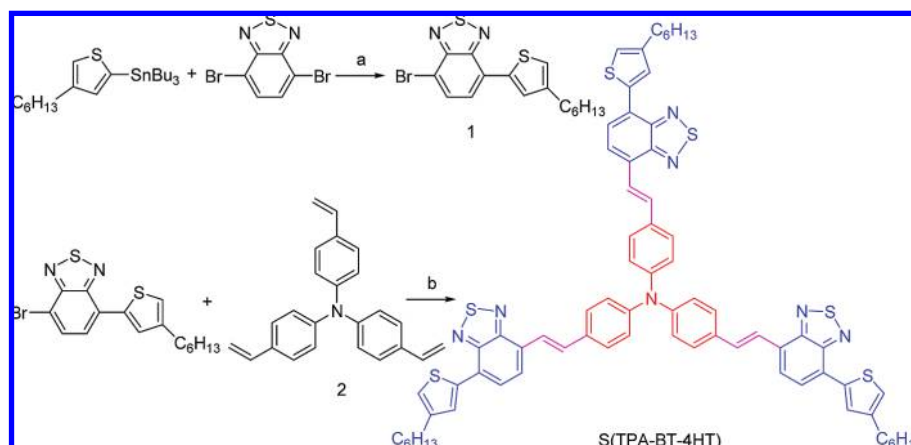
S(TPA-BT-4HT) is soluble in common organic solvents, such as CHCl<sub>3</sub>, THF, chlorobenzene, and toluene. The thermal stability of the compound was investigated by thermogravimetric analysis (TGA). The temperature with 5% weight loss is at 303 °C, as shown in Figure S1 in the Supporting Information. The stability of S(TPA-BT-4HT) is enough for the applications in optoelectronic devices.

Figure 1 shows the UV–vis absorption and photoluminescent (PL) spectra of S(TPA-BT-4HT) in chloroform solution and film state. Benefited from its D–A molecular structure connected with conjugated bridge, the absorption spectrum of S(TPA-BT-4HT) in chloroform solution exhibits strong absorption in the wavelength range from 300 to 600 nm with three peaks at 316, 361, and 509 nm. The UV absorption with a maximum at 316 and 361 nm corresponds to the  $\pi$ – $\pi^*$  absorption of the molecule, and the visible absorption band with a peak at 509 nm could be assigned to the intramolecular charge transfer transition between the TPA moiety and BT unit. In comparison with dilute solution, the three absorption peaks of S(TPA-BT-4HT) film red-shifted a little, which are at 320, 370, and 529 nm. The red shift of the absorption peaks of the film indicates some aggregation of the molecules in the film state existed. The absorption edge of S(TPA-BT-4HT) film is at ca. 631 nm, corresponding to a bandgap of 1.96 eV. Actually, the absorption spectrum of S(TPA-BT-4HT) is quite similar to that of S(TPA-BT).<sup>15</sup> As the photovoltaic organic molecule, the absorption strength of the organic molecule films is a key parameter for better utility of solar light. The peak absorbance of the S(TPA-BT-4HT) film with a thickness of ca. 100 nm is  $1.21 \times 10^{-2} \text{ nm}^{-1}$ , which is ca. 20% increased in comparison with that ( $1.04 \times 10^{-2} \text{ nm}^{-1}$ ) of the S(TPA-BT) film;<sup>15</sup> PL spectra of S(TPA-BT-4HT) in chloroform solution and in film show a red emission with a peak at ca. 656 and 657 nm, respectively, as also shown in Figure 1.

Electrochemical cyclic voltammetry was carried out for the S(TPA-BT-4HT) film on a glassy carbon electrode, in order to measure the HOMO and LUMO energy levels of S(TPA-BT-4HT). Figure 2 shows the cyclic voltammogram of the S(TPA-BT-4HT) film. It can be seen that the onset reduction potential ( $E_{\text{onset}}^{\text{red}}$ ) of the compound is at  $-1.63 \text{ V}$  vs Ag/Ag<sup>+</sup>, and the onset oxidation potential ( $E_{\text{onset}}^{\text{ox}}$ ) is at  $0.48 \text{ V}$  vs Ag/Ag<sup>+</sup>. The HOMO and LUMO energy levels and the electrochemical band gap were estimated to be  $-5.19$ ,  $-3.08$ , and  $2.11 \text{ eV}$ , respectively, from the onset oxidation and reduction potentials according to the following equations:<sup>25</sup>  $E_{\text{HOMO}} = -e(E_{\text{onset}}^{\text{ox}} + 4.71) \text{ (eV)}$ ,  $E_{\text{LUMO}} = -e(E_{\text{onset}}^{\text{red}} + 4.71) \text{ (eV)}$ , and  $E_g = E_{\text{LUMO}} - E_{\text{HOMO}}$ .

Bulk-heterojunction OSCs were fabricated by using S(TPA-BT-4HT) as donor, [70]PCBM as acceptor,<sup>26–29</sup> and Al or Mg/Al as the negative electrode. The device structure is ITO/PEDOT:PSS/photoactive layer (60 nm)/Al or Mg/Al. The weight ratio of S(TPA-BT-4HT):[70]PCBM in the photoactive layer was optimized to be 1:3. As shown in AFM images (see Figure S2 in Supporting Information), compared with the 1:3 (w/w) S(TPA-BT):[60]PCBM blend film<sup>15</sup> and the 1:1 (w/w) S(TPA-BT-4HT):[70]PCBM blend film, the 1:3 (w/w) S(TPA-BT-4HT):[70]PCBM blend film shows better film morphology.

\*Corresponding author: E-mail liyf@iccas.ac.cn, Fax 86-10-62559373.

Scheme 1. Synthetic Route of S(TPA-BT-4HT)<sup>a</sup>

<sup>a</sup> Conditions: (a) Pd(PPh<sub>3</sub>)<sub>2</sub>Cl<sub>2</sub>, THF, N<sub>2</sub>, reflux for 24 h; (b) Pd(OAc)<sub>2</sub>, NaOAc, *n*-Bu<sub>4</sub>NBr, DMF, N<sub>2</sub>, reflux for 24 h.

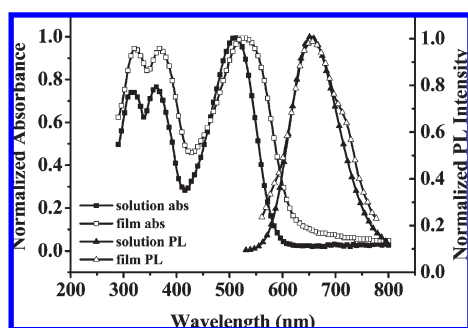


**Figure 1.** UV-vis absorption and PL spectra of TPA-BT-4HT in chloroform solution and in film state. The PL spectra were taken by excitation at 325 nm.

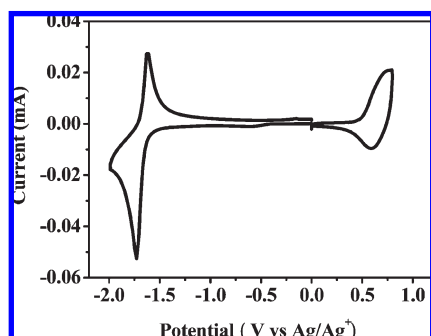


**Figure 2.** Cyclic voltammogram of TPA-BT-4HT film on glassy carbon electrode in an acetonitrile solution of 0.1 mol/L Bu<sub>4</sub>NPF<sub>6</sub> (Bu = butyl) with a scan rate of 100 mV/s.

It reveals that S(TPA-BT-4HT) has better film-forming properties than S(TPA-BT),<sup>15</sup> and the 1:3 weight ratio of S(TPA-BT-4HT): [70]PCBM is better in the fabrication of the OSCs from the viewpoint of morphology.

Figure 3 shows the typical current-voltage curves of the OSCs at dark and under the illumination of AM 1.5, 100 mW/cm<sup>2</sup>. The device with Al as negative electrode demonstrated an open-circuit voltage ( $V_{oc}$ ) of 0.87 V, a short-circuit current ( $I_{sc}$ ) of 6.01 mA/cm<sup>2</sup>, and a fill factor (FF) of 40.1%, corresponding to a power conversion efficiency (PCE) of 2.10%. By using a Mg/Al as negative electrode, the  $I_{sc}$  of the device was improved to 8.58 mA/cm<sup>2</sup>, with a  $V_{oc}$  of 0.85 V and a FF of 32.7%, producing a PCE of 2.39%. It is well-known that in the thin film OSCs the

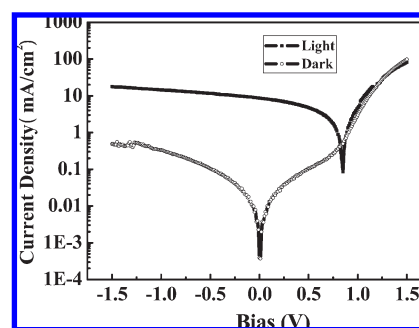


**Figure 3.** Current density-voltage characteristics of the OSC device based on the blend of S(TPA-BT-4HT)/[70]PCBM (1:3, w/w) with Mg/Al as the negative electrode at dark and under the illumination of AM 1.5, 100 mW/cm<sup>2</sup>.

driving force for charge migration is considered to be the internal electric field produced by the work function difference of the positive and negative electrode.<sup>30</sup> Therefore, the lower work function of the Mg/Al electrode should be beneficial to the improvement of the  $I_{sc}$  and PCE of the device. The improved photovoltaic performance of S(TPA-BT-4HT) in comparison with that of S(TPA-BT)<sup>15</sup> could benefit from its stronger absorbance, better morphology of its blend film, and better visible absorption of [70]PCBM than PCBM. The  $I_{sc}$  of 8.58 mA/cm<sup>2</sup> and PCE of 2.39% are among the highest values in the OSCs based on solution-processable organic molecules reported so far. The results indicate that the solution processable organic molecules are also promising for high-efficiency solar cells.

In conclusion, a star-shaped solution processable organic molecule with TPA as core and BT-4HT as arms, S(TPA-BT-4HT), was designed and synthesized for the application in the solution-processed OSCs. S(TPA-BT-4HT) film shows broad and strong absorption peaks in the range of 300–630 nm and a red-emission photoluminescent peak at ca. 657 nm. The OSC devices were fabricated by spin-coating the blend solution of S(TPA-BT-4HT) as donor and [70]PCBM as acceptor. The OSC device based on a blend of S(TPA-BT-4HT) and [70]PCBM (1:3, w/w) exhibited an  $I_{sc}$  of 8.58 mA/cm<sup>2</sup>, a  $V_{oc}$  of 0.85 V, and a FF of 32.7%, corresponding to a PCE of 2.39%, under the illumination of AM 1.5, 100 mW/cm<sup>2</sup>. The  $I_{sc}$  of 8.58 mA/cm<sup>2</sup> and PCE of 2.39% are among the highest values for the OSCs based on the solution-processable organic molecules reported so far.

**Experimental Section.** *Chemicals.* 3-Hexylthiophene, *n*-butyllithium (2.88 mol/L in hexane), tri-*n*-butyltin chloride, 4,7-dibromo-2,1,3-benzothiadiazole, Pd(PPh<sub>3</sub>)<sub>2</sub>Cl<sub>2</sub>, tetrabutylammonium bromide, sodium acetate, palladium acetate, and DMF were obtained from Acros Organics. Tetrahydrofuran (THF) was dried over Na/benzophenone ketyl and freshly distilled prior to use. Monomer **2** was synthesized as reported in the literature.<sup>21</sup> Other chemicals were common commercial level and were used as received.

*Measurements.* Nuclear magnetic resonance (NMR) spectra were taken on a Bruker DMX-400 spectrometer. MALDI-TOF spectra were recorded on a Bruker BIFLEXIII. Absorption spectra were taken on a Hitachi U-3010 UV-vis spectrophotometer. PL spectra were measured using a Hitachi F-4500 spectrophotometer. The film on quartz used for UV measurements was prepared by spin-coating with 1% chloroform solution. The TGA measurement was performed on a Perkin-Elmer TGA-7 apparatus. The electrochemical cyclic voltammogram was obtained using a Zahner IM6e electrochemical workstation in a 0.1 mol/L tetrabutylammonium hexafluorophosphate (Bu<sub>4</sub>NPF<sub>6</sub>)-acetonitrile solution. A glassy carbon electrode coated with the sample film was used as the working electrode; a Pt wire and Ag/Ag<sup>+</sup> (0.01 M AgNO<sub>3</sub> in acetonitrile) were used as the counter and reference electrodes, respectively.

*Fabrication and Characterization of Organic Solar Cells.* Organic solar cells (OSCs) were fabricated in the configuration of the traditional sandwich structure with an ITO positive electrode and a metal negative electrode. Patterned ITO glass with a sheet resistance of 30 Ω □<sup>-1</sup> was purchased from CSG Holding Co., Ltd. (China). The ITO glass was cleaned in an ultrasonic bath of acetone and isopropanol and treated by UVO (ultraviolet ozone cleaner, Jelight Co.). Then a thin layer (30 nm) of PEDOT:PSS (poly(3,4-ethylenedioxythiophene)-poly(styrenesulfonate)) (Baytron PVP A1 4083, Germany) was spin-coated on the ITO glass. Subsequently, the photosensitive layer was prepared by spin-coating the blend solution of S(TPA-BT-4HT) and [70]PCBM (1:3 w/w) on the top of the PEDOT:PSS layer (ca. 60 nm thickness) and baked at 80 °C for 0.5 h. The concentration of the solution was 10 mg/mL in chlorobenzene. The thickness of the photoactive layer was measured using an Ambios Technology XP-2 profilometer. Finally, a metal electrode layer of Al (ca. 120 nm) or a layer of Mg (ca. 8 nm) capped with Al (ca. 120 nm) was vacuum-evaporated on the photoactive layer under a shadow mask in the vacuum of ca. 10<sup>-4</sup> Pa. The current-voltage (*I*-*V*) measurement of the devices was conducted on a computer-controlled Keithley 236 Source Measure Unit. A xenon lamp coupled with A.M. 1.5 solar spectrum filters was used as light source, and the optical power at the sample was ca. 100 mW/cm<sup>2</sup>.

#### Synthesis

##### 4-Bromo-7-(4-hexyl-2-thienyl)-2,1,3-benzothiadiazole.

Under a nitrogen atmosphere, a mixture of 4,7-dibromo-2,1,3-benzothiadiazole (27.78 g, 94.49 mmol), tributyl-(4-hexyl-2-thienyl)stannane (35.9 g, 78.74 mmol), and Pd(PPh<sub>3</sub>)<sub>2</sub>Cl<sub>2</sub> (552 mg, 0.79 mmol) was dissolved in degassed anhydrous THF (250 mL). The solution was kept at 80 °C for 24 h. The mixture was poured into water and extracted with dichloromethane. The organic layer was washed with brine and then dried over anhydrous sodium sulfate. After evaporation of the solvent, the residue was purified by column chromatography on silica gel (eluent petroleum/CH<sub>2</sub>Cl<sub>2</sub>, 10:1). Recrystallization from ethanol gave the pure product as yellow solid with a yield of 33.3%; mp 61.41 °C. MS: *m/z* = 382 (M<sup>+</sup>). <sup>1</sup>H NMR (CDCl<sub>3</sub>, 400 MHz): δ [ppm] 7.96 (s, 1H), 7.84 (d, 1H), 7.70 (d, 1H), 7.07 (s, 1H), 2.71 (t, 2H),

1.73 (m, 2H), 1.41 (m, 2H), 1.3 (m, 4H), 0.92 (t, 3H). <sup>13</sup>C NMR (CDCl<sub>3</sub>, 400 MHz): δ [ppm] 153.75, 151.73, 144.46, 138.06, 132.28, 129.60, 127.29, 125.45, 122.03, 112.02, 31.69, 30.60, 30.44, 29.03, 22.63, 14.10.

*Tris(4-(2-(7-(4-hexyl-2-thienyl)-2,1,3-benzothiadiazol-4-yl)-vinyl)phenyl)amine, S(TPA-BT-4HT).* A mixture of tris(4-vinylphenyl)amine (256 mg, 0.79 mmol), Pd(OAc)<sub>2</sub> (5 mg), NaOAc (1.90 g, 23.8 mmol), 4-bromo-7-(4-hexyl-2-thienyl)-2,1,3-benzothiadiazole (1 g, 2.62 mmol), and *n*-Bu<sub>4</sub>NBr (123 mg, 0.38 mmol) was dissolved in degassed *N,N*-dimethylformamide (DMF) (50 mL). The solution was kept under a nitrogen atmosphere at 100 °C for 24 h. The mixture was poured into water. The precipitate was filtered, washed with water and dissolved in dichloromethane, and dried over anhydrous sodium sulfate. After evaporation of the solvent, the residue was purified by column chromatography on silica gel (eluent petroleum/CH<sub>2</sub>Cl<sub>2</sub>, 2:1) to produce 300 mg of red solid of S(TPA-BT-4HT) with a yield of 30%. MALDI-TOF MS: 1223.3, calcd for C<sub>72</sub>H<sub>69</sub>N<sub>7</sub>S<sub>6</sub> 1223.0. <sup>1</sup>H NMR (CDCl<sub>3</sub>, 400 MHz): δ [ppm] 7.97 (d, 6H), 7.78 (d, 3H), 7.65 (d, 3H), 7.58 (d, 6H), 7.53 (d, 3H), 7.19 (d, 6H), 7.02 (s, 3H), 2.71 (t, 6H), 1.72 (m, 6H), 1.40 (m, 18H), 0.90 (t, 9H). <sup>13</sup>C NMR (CDCl<sub>3</sub>, 400 MHz): δ [ppm] 153.88, 152.76, 147.00, 144.38, 139.25, 132.58, 132.50, 129.28, 128.96, 128.00, 126.50, 126.00, 125.67, 124.38, 123.20, 121.47, 31.73, 30.69, 30.50, 29.72, 22.66, 14.13.

**Acknowledgment.** This work was supported by NSFC (Nos. 50633050, 50803071, 20874106, and 20721061).

**Supporting Information Available:** TGA and AFM images of S(TPA-BT-4HT). This material is available free of charge via the Internet at <http://pubs.acs.org>.

#### References and Notes

- (1) Ma, C.-Q.; Mena-Osteritz, E.; Debaerdemaeker, T.; Wienk, M. M.; Janssen, R. N. J.; Bauerle, P. *Angew. Chem., Int. Ed.* **2007**, *46*, 1679–1683.
- (2) Ma, C.-Q.; Fonrodona, M.; Schikora, M. C.; Wienk, M. M.; Janssen, R. A. J.; Bauerle, P. *Adv. Funct. Mater.* **2008**, *18*, 3323–3331.
- (3) Cremer, J.; Bauerle, P. *J. Mater. Chem.* **2006**, *16*, 874–884.
- (4) Kopidakis, N.; Mitchell, W. J.; van de Lagemaat, J.; Ginley, D. S.; Rumbles, G.; Shaheen, S. E. *Appl. Phys. Lett.* **2006**, *89*, 103524.
- (5) Sun, X.; Zhou, Y.; Wu, W.; Liu, Y.; Tian, W.; Yu, G.; Qiu, W.; Chen, S.; Zhu, D. *J. Phys. Chem. B* **2006**, *110*, 7702–7707.
- (6) Shirota, Y.; Kageyama, H. *Chem. Rev.* **2007**, *107*, 953–1010.
- (7) Roquet, S.; Bettignies, de R.; Leriche, P.; Cravino, A.; Roncali, J. *J. Mater. Chem.* **2006**, *16*, 3040–3045.
- (8) Cravino, A.; Roquet, S.; Aleveque, O.; Leriche, P.; Frere, P.; Roncali, J. *J. Chem. Mater.* **2006**, *18*, 2584–2590.
- (9) Roquet, S.; Cravino, A.; Leriche, P.; Aleveque, O.; Frere, P.; Roncali, J. *J. Am. Chem. Soc.* **2006**, *128*, 3459–3466.
- (10) Roncali, J.; Leriche, P.; Cravino, A. *Adv. Mater.* **2007**, *19*, 2045–2060.
- (11) Sun, M.; Wang, L.; Zhu, X.; Du, B.; Liu, R.; Yang, W.; Cao, Y. *Sol. Energy Mater. Sol. Cells* **2007**, *91*, 1681–1687.
- (12) Silvestri, F.; Irwin, M. D.; Beverina, L.; Facchetti, A.; Pagani, G. A.; Marks, T. J. *J. Am. Chem. Soc.* **2008**, *130*, 17640–17641.
- (13) Tamayo, A. B.; Walker, B.; Nguyen, T.-Q. *J. Phys. Chem. C* **2008**, *112*, 11545–11551.
- (14) Tamayo, A. B.; Dang, X.-D.; Walker, B.; Seo, J.; Kent, T.; Nguyen, T.-Q. *Appl. Phys. Lett.* **2009**, *94*, 103301.
- (15) He, C.; He, Q.; Yi, Y.; Wu, G.; Bai, F.; Shuai, Z.; Li, Y. F. *J. Mater. Chem.* **2008**, *18*, 4085–4090.
- (16) Shirota, Y. *J. Mater. Chem.* **2000**, *10*, 1–25.
- (17) Shirota, Y. *J. Mater. Chem.* **2005**, *15*, 75–93.
- (18) Zheng, L.; Urian, R. C.; Liu, Y. Q.; Jen, A. K. Y.; Pu, L. *Chem. Mater.* **2000**, *12*, 13–15.
- (19) Zhou, Y.; He, Q.; Yang, Y.; Zhong, H.; He, C.; Yang, C.; Liu, W.; Bai, F.; Li, Y. F. *Adv. Funct. Mater.* **2008**, *18*, 3299–3306.

- (20) He, C.; He, Q.; He, Y.; Li, Y.; Bai, F.; Yang, C.; Ding, Y.; Wang, L.; Ye, J. *Sol. Energy Mater. Sol. Cells* **2006**, *90*, 1815–1827.
- (21) Wu, G.; He, C.; Zhang, J.; He, Q.; Chen, X.; Li, Y. *Sol. Energy Mater. Sol. Cells* **2009**, *93*, 108–113.
- (22) He, C.; He, Q.; Yang, X.; Wu, G.; Yang, C.; Bai, F.; Shuai, Z.; Wang, L.; Li, Y. *J. Phys. Chem. C* **2007**, *111*, 8661–8666.
- (23) Zhao, G.; Wu, G.; He, C.; Bai, F.; Xi, H.; Zhang, H.; Li, Y. *J. Phys. Chem. C* **2009**, *113*, 2636–2642.
- (24) Hou, Q.; Zhou, Q.; Zhang, Y.; Yang, W.; Yang, R.; Cao, Y. *Macromolecules* **2004**, *37*, 6299–6305.
- (25) Sun, Q.; Wang, H.; Yang, C.; Li, Y. *J. Mater. Chem.* **2003**, *13*, 800–806.
- (26) Wienk, M. M.; Kroon, J. M.; Verhees, W. J. H.; Knol, J.; Hummelen, J. C.; van Hal, P. A.; Janssen, R. A. J. *Angew. Chem., Int. Ed.* **2003**, *42*, 3371–3375.
- (27) Kooistra, F. B.; Mihailetchi, V. D.; Popescu, L. M.; Kronholm, D.; Blom, P. W. M.; Hummelen, J. C. *Chem. Mater.* **2006**, *18*, 3068–3073.
- (28) Hou, J.; Chen, H.; Zhang, S.; Li, G.; Yang, Y. *J. Am. Chem. Soc.* **2008**, *130*, 16144–16145.
- (29) Thompson, B. C.; Frechet, J. M. J. *Angew. Chem., Int. Ed.* **2008**, *47*, 58–77.
- (30) Brabec, C. J. *Sol. Energy Mater. Sol. Cells* **2004**, *83*, 273–292.